Statistical characterization of spatial transfiguration of waveforms recorded in some recent crustal earthquakes in Japan

Yuichi MASUDA[1] and Tsuyoshi TAKADA[2]

[1] *Graduate Student, Graduate School of Engineering, the University of Tokyo, Tokyo, Japan*
[2] *Professor, Graduate School of Engineering, the University of Tokyo, Tokyo, Japan*
Email: masuda@load.arch.t.u-tokyo.ac.jp, takada@load.arch.t.u-tokyo.ac.jp

ABSTRACT :

Up to now, empirical estimation of ground motion has been proposed as an attenuation relation for IM(Intensity Measure) of ground motion, peak intensity or response spectrum generally. The most important thing about this study is that not only intensity characteristics but also temporal characteristics are taken into consideration. Modeling RMS envelopes with some IMs, examining attenuation or augmentation relations by regression analysis with simple regression formula, studying the correlation structure of the residual among the IMs or frequency bands with principal component analysis, and finally, the perspective that the residuals can be explained with physical quality such as soil conditions or propagation to some extent is shown.

KEYWORDS: Empirical estimation, Envelope of waveform, Bandwidth division
Crustal earthquakes, Correlation structure, Principle component analysis

1. Introduction

Strong ground motion predictions using characterized source models and their applications have been continuing their remarkable development. On the other hand, empirical ground motion attenuation relations have been widely adopted to provide a median value and uncertainty of prediction for the probabilistic seismic hazard analysis. In this regard, however, Intensity measures of ground motion such as peak intensities including PGA, PGV and PGD or response spectrum are considered as the IM representing the hazard at a site as usual.

Time history is a perfect form representing ground motion. It is desirable that the waveform at each site can be predicted to some extent on the condition that the specific structure of the fault is unknown. The main purpose of this study is to model the time-dependent waveform of the ground motion at sites for large earthquakes, intending nonlinear response of structures. In this paper, observations recorded in some recent crustal earthquakes in Japan are analyzed by statistical-analytical approach.

2. Method of analysis

2.1. Observation Records for Analysis

In this study, strong motion observations recorded at K-NET and KiK-NET stations were used. Acceleration records in the 24 events were chosen for the following criteria. (1) Recent crustal earthquakes the hypo central depths of which are shallower than 20 km. (2) Their Moment magnitudes M_W are more than 5.5. Basic information of the earthquakes is shown in Table 1. As waveform as well as intensity is affected by soil conditions, Strong motion records on the surface are converted to those on engineering bedrock (S-wave velocity V_S = 500 km/sec) using SHAKE program. So and from the standpoint of engineering utilization, the records used for analysis was limited for the following rules. (1) Hypo central distance is less than 150 km (2) S-wave velocity structure necessary for the strip off inversion analysis is well known.

2.2. Calculation of Band-limited Envelope of Waveform

First, each of 3 components (EW, NS, UD) of acceleration records was devided into frequency bands using discrete wavelet transform as below.

$$f_0(t) = g_{-1}(t) + g_{-2}(t) + \cdots + g_{-n}(t) + f_{-n}(t) \tag{2.1}$$

Here, n is called 'level' of wavelet decomposition, $f_n(t)$ and $g_{-j}(t)(j = 1,2,\ldots,n)$ are called 'approximation' and 'detail', respectively. Correspondence relation of level j and frequency band T_j is to be

Table 1 Earthquakes records of which are used for analysis

No.	Year	M.	D.	Region	Lat(°)	Long(°)	Depth(km)	Mw	Sites
1	1996	8	11	SOUTHERN_AKITA_PREF	140.65	39.00	9	6	81
2	1996	8	11	NORTHERN_MIYAGI_PREF	140.69	38.71	10	5.7	90
3	1997	3	26	NW_KAGOSHIMA_PREF	130.33	31.99	12	6.1	113
4	1997	4	3	NW_KAGOSHIMA_PREF	130.29	31.96	15	5.5	63
5	1997	5	13	NW_KAGOSHIMA_PREF	130.29	32.02	9	6.2	103
6	1997	6	25	YAMAGUCHI_PREF	131.66	34.41	8	5.9	155
7	1998	5	3	E_OFF_IZU_PENINSULA	139.19	34.85	5	5.6	76
8	1998	8	16	HIDA_MOUNTAINS_REGION	137.60	36.32	3	5.5	51
9	1998	9	3	NORTHERN_IWATE_PREF	140.90	39.76	8	5.9	65
10	2000	7	15	NEAR_NIIJIMA_ISLAND	139.25	34.47	10	6.1	73
11	2000	10	3	FAR_E_OFF_SANRIKU	143.40	40.01	10	6.1	46
12	2000	10	6	WESTERN_TOTTORI_PREF	133.37	35.16	9	6.8	198
13	2003	7	26	NORTHERN_MIYAGI_PRE	141.16	38.62	12	6.1	135
14	2004	10	23	MID_NIIGATA_PRE	138.88	37.30	13	6.7	256
15	2004	10	23	MID_NIIGATA_PRE	138.93	37.33	14	6.4	246
16	2004	10	25	MID_NIIGATA_PRE	138.95	37.37	15	5.7	179
17	2004	10	27	MID_NIIGATA_PRE	139.04	37.26	12	6	222
18	2004	11	8	MID_NIIGATA_PRE	139.05	37.30	0	5.6	156
19	2004	12	14	RUMOI_REGIO	141.71	44.23	9	5.8	70
20	2005	3	20	NW_OFF_KYUSHU	130.17	33.74	9	6.7	157
21	2005	4	20	CENTRAL_FUKUOKA_PREF	130.29	33.77	14	5.5	135
22	2006	4	21	E_OFF_IZU_PENINSULA	139.21	34.78	7	5.5	119
23	2007	3	25	OFF_NOTO_PENINSUL	136.66	37.16	11	6.6	157
24	2007	7	16	OFF_S_NIIGATA_PRE	138.60	37.44	17	6.7	239

$$T_j = 2^j \Delta t \sim 2^{j+1} \Delta t \,. \tag{2.2}$$

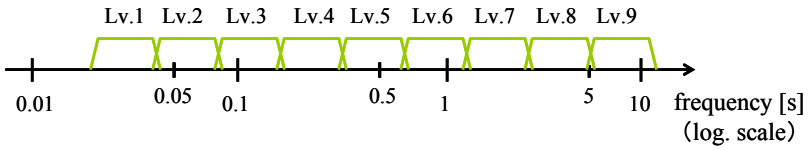

Figure 2.1 Levels and Frequency Bands

In this study, Δt = 0.01 sec. Daubechies's wavelet function (N = 10) was adopted as the mother wavelet $\Psi(t)$. Then, details were calculated up to level 8 so that the approximation was small enough to ignore. Next, RMS envelopes were calculated as

$$e_j(t) = \sqrt{\frac{1}{2\Delta T}\int_{t-\Delta T}^{t+\Delta T}\left[\{x_{EW,j}(t)\}^2 + \{x_{NS,j}(t)\}^2 + \{x_{UD,j}(t)\}^2\right]dt} \,. \tag{2.3}$$

Here, ΔT is the central frequency of the band. Although ground motion waveforms generally vary, are affected by nonhomogeneity of propagation path, RMS envelope is said to be a site-specific stable quantity. This RMS envelope at each level is the central interest of this study, and it is the main objective to study an empirical model of RMS envelope.

2.3. Parameterization of Band-limited Envelope

In order to estimate envelopes empirically, envelope of each level is modeled in terms of intensity measure and temporal measures. First, total acceleration power was adopted as the intensity measure and calculated for each record, because acceleration power is said to be related to elastic-plastic response of systems. Total acceleration power is the time integration of the square of acceleration shown as below

$$I_j = \int_0^{T_0} \{e_j(t)\}^2 dt \,. \tag{2.4}$$

Secondly, temporal measures were chosen, assuming an envelope as a distribution profile. To be more precise, the time corresponding to the gravity point of the distribution is defined as t_g, standard deviation, skewness and kurtosis about the center of gravity are defined as σ_T, β_T and γ_T, respectively. Those are,

$$t_{go} = t_g - t_o, \quad t_g = \frac{\int_0^{T_0} t \cdot e(t) dt}{\int_0^{T_0} e(t) dt} \tag{2.5}$$

$$\sigma_T = \sqrt{\mu_2}, \quad \beta_T = \frac{\mu_3}{\sigma_T^{\,3}}, \quad \gamma_T = \frac{\mu_4}{\sigma_T^{\,4}} - 3 \tag{2.6}$$

Here, nth-order moment with respect to the center of gravity is

$$\mu_n = \frac{\int_{t_1}^{t_{95}} (t - t_g)^n \cdot e(t) dt}{\int_{t_1}^{t_{95}} e(t) dt} \,. \tag{2.7}$$

σ_T, broadening on time axis has a unit of time (second), β_T and γ_T are dimensionless IMs characterizing envelope shape.

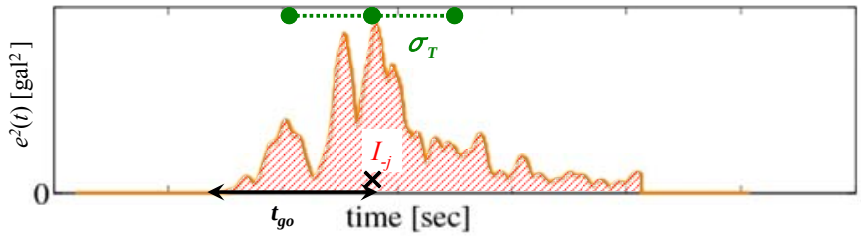

Figure 2.2 IMs Characterizing Envelope Shape

2.4. Regression Model

For each objective variable, regression analysis was done in which hypo central distance was explaining variable. Then, the regression model below is used, in case that an objective variable is I, t_{go} or σ_T,

$$\log_{10} P = c_1 + c_2 \log_{10}(X + c_3) \quad \Leftrightarrow \quad P = c_1'(X + c_3)^{c_2}, \quad c_1' = 10^{c_1} \,. \tag{2.8}$$

when objective variable is β_T or γ_T

$$P = c_1 + c_2 X \,. \tag{2.9}$$

Here, P means objective variable c_1,c_2 and c_3 are regression coefficients.

3. Result of Calculations

3.1. Attenuation or Augmentation Relations for Objective Variables

Figure 3.1 describes one series of results of regression analysis (Niigata Chuetsu Earthquake main shock), Figure 3.2 shows Mean Values of the IMs for some earthquakes, and standard deviation of regression analysis is in Table3.1. The graph of I shows what is called attenuation relation, standard deviation of which is 0.55(common logarithm). The graphs of t_{go} and σ_T show value augmentation of the objective variables, the curve fitting to the data very well and their uncertainties are very small. The graph of β_T shows that farther from the hypocenter, more negative β_T is, and implies that there is still room for improvement of regression formula. The graph of γ_T shows that the value increases or decreases with distance from the hypo central depending on earthquakes.

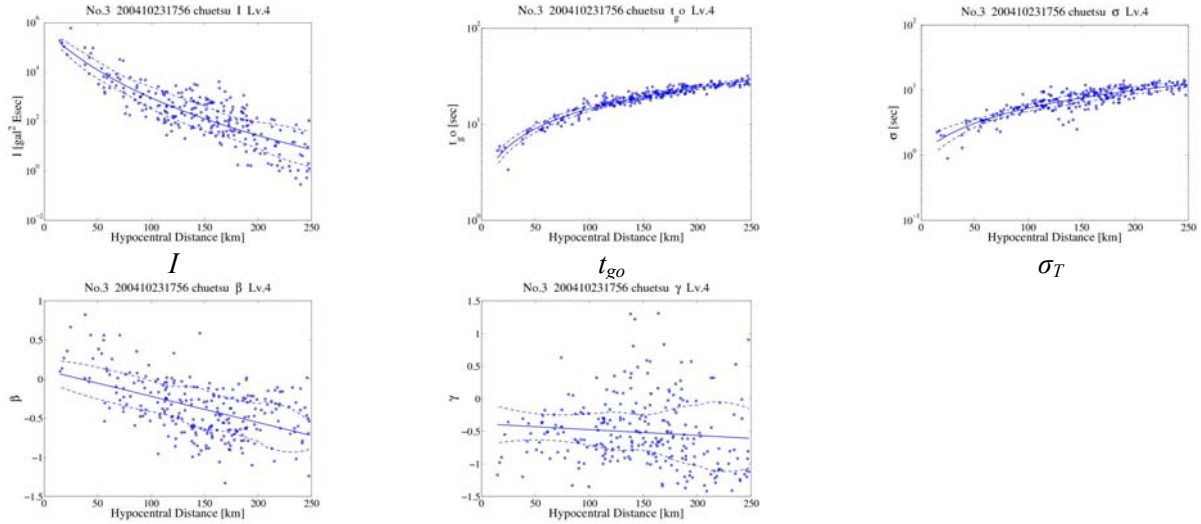

I t_{go} σ_T

β_T γ_T

Figure 3.1 an Example of Regression Analysis (Niigata Chuetsu Earthquake Main Shock)

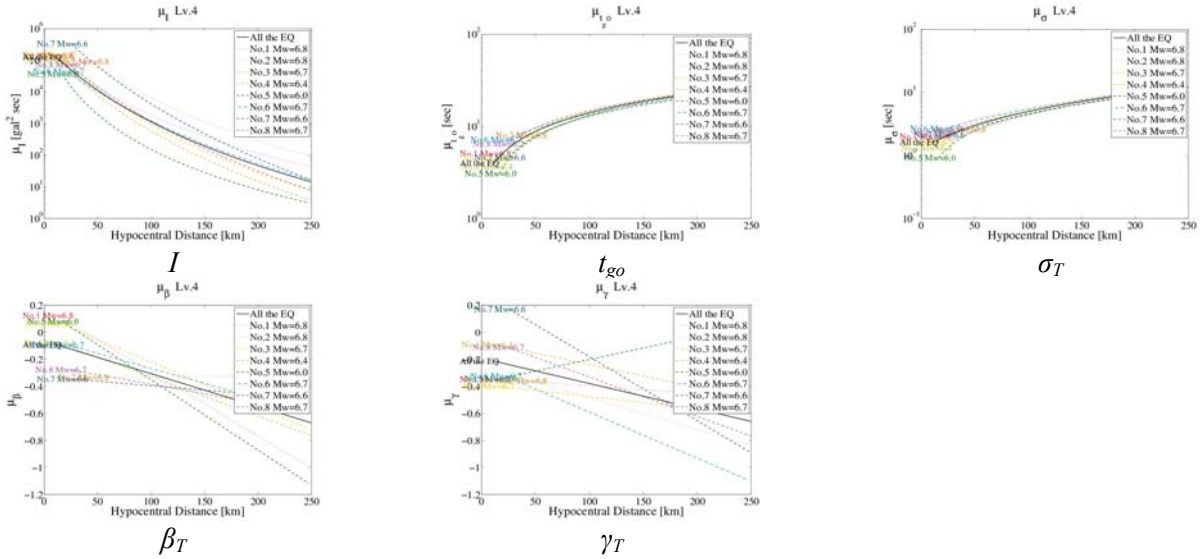

I t_{go} σ_T

β_T γ_T

Figure 3.2 Mean Value of the IM

Table 3.1 Standard Deviation of Regression Analysis

I	t_{go}	σ_T,	β_T	γ_T
0.55	0.04	0.08	0.35	0.49

The maps in Figure 3.3 show the residual of each site for Lv.4 envelopes by Niigata Chuetsu Earthquake Main Shock. Each IM is to be correlated because the waveform is to transform gradually with the distance from the hypo centre affected by refraction or scattering. So, in the next section, correlation structureof the residuals is analyzed using principal component analysis, aiming to relate principal modes with soil conditions or propagation path.

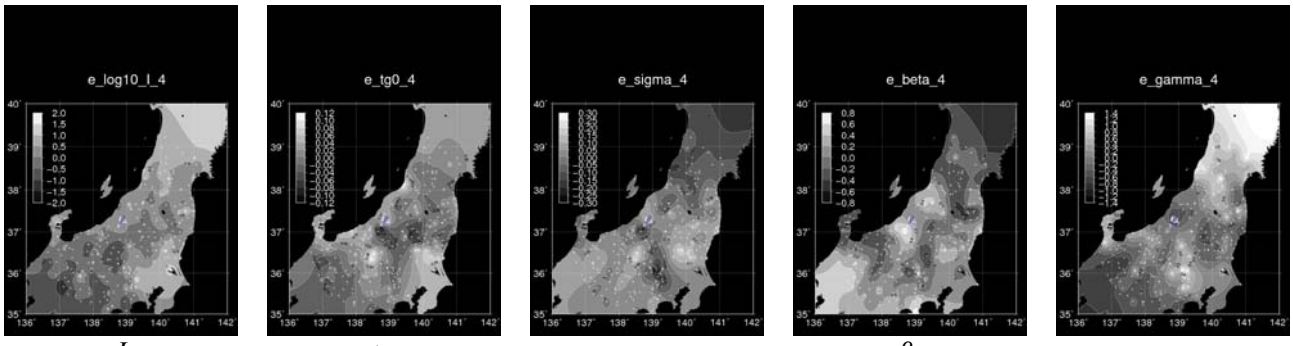

I t_{go} σ_T β_T γ_T

Figure 3.3 Mapping of Residual (Niigata Chuetsu Earthquake Main Shock, Lv.4)

3.2. Correlation Structure of Residuals

Figure 3.4 shows an example of correlation structure among IMs and among Levels (Niigata Chuetsu Earthquake Main Shock). White circles mean positive correlation and black ones means negative. For example looking at the figure at the left side, it is found that I has negative correlation with σ_T, though it may be small. It means that waves like pulse are apt to have bigger energy than lengthy waves. The figure at the right side shows it that residuals in nearer frequencies bands have higher positive correlation, at least about I.

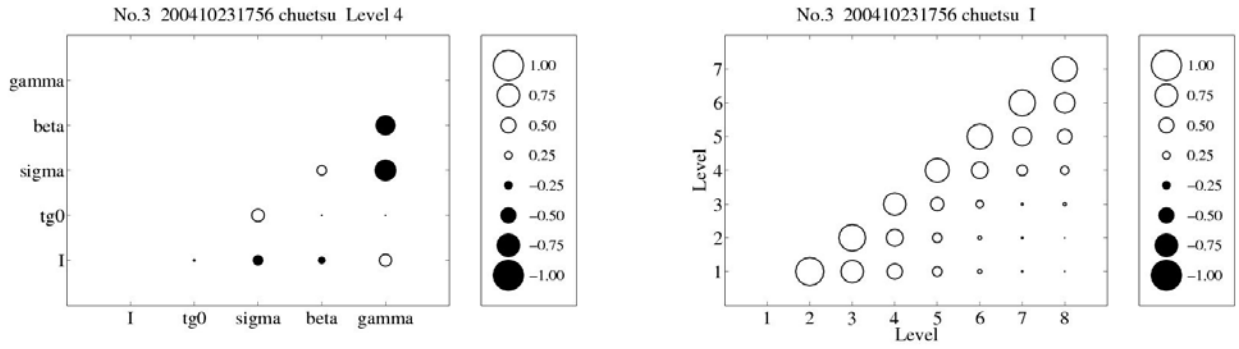

Among IMs(Chuetsu Earthquake, Lv.4) Among Levels(Chuetsu Earthquake, I)

Figure 3.4 an Example of Correlation Structure

Using principal component analysis, those correlation structures were decomposed. Figure 3.5 shows cumulative proportion of each principal mode for some earthquakes. For example, over 80% of the correlation structure among IMs (in Level4) is found to be accounted for by the top 3 principal components. Similarly, it can be said that over 70% of the correlation structure among levels (for I) is explained by the top 2 principal components and over 80%, of that, by the top 3. This tendency was also true of all levels and IMs.

So, the top 3 principal components are examined about the correlation structure for each IM or level. A set of example (Niigata Chuetsu Earthquake Main Shock, among IMs for Level 4 or among Levels for each IM) is described in Fig3.6.

First, looking at the shapes of principal modes for the correlation structure among IMs, mode 1 is a component

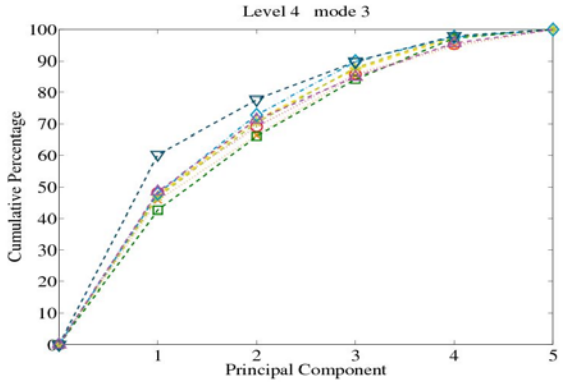

Among IMs(Chuetsu Earthquake, Lv.4)

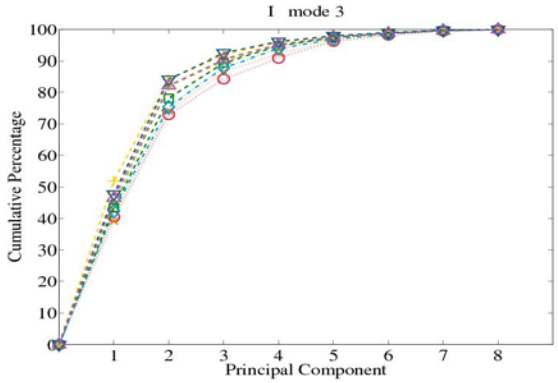

Among Levels(Chuetsu Earthquake, *I*)

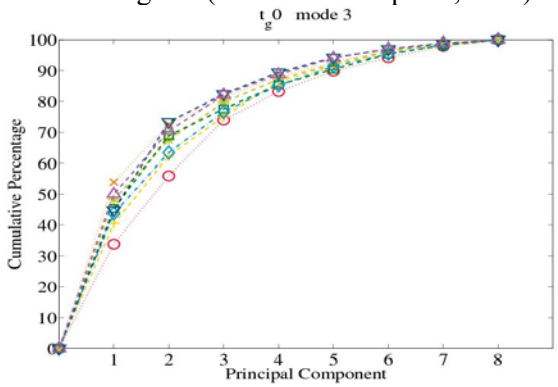

Among Levels(Chuetsu Earthquake, t_{go})

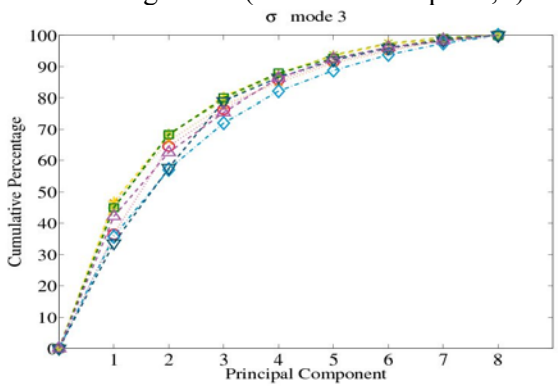

Among Levels(Chuetsu Earthquake, σ_T)

Figure 3.5 an Example of Cumulative Proportion of Each Principal Mode

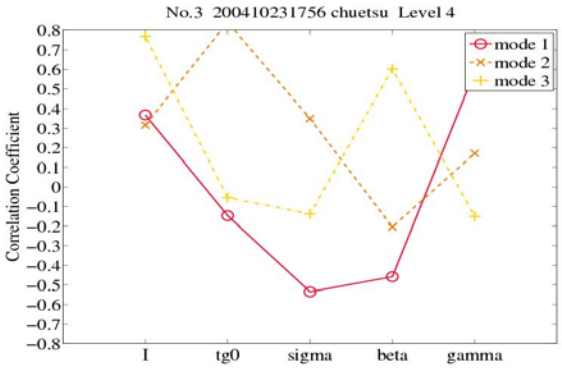

Among IMs(Chuetsu Earthquake, Lv.4)

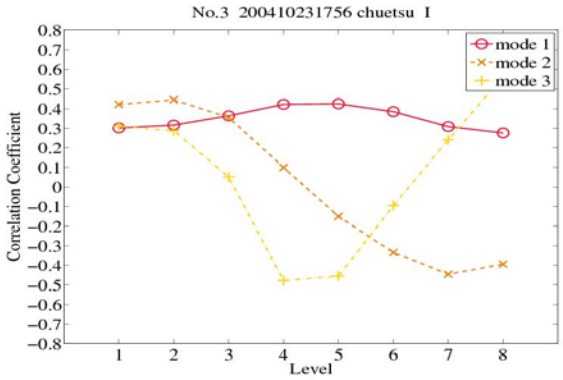

Among Levels(Chuetsu Earthquake, *I*)

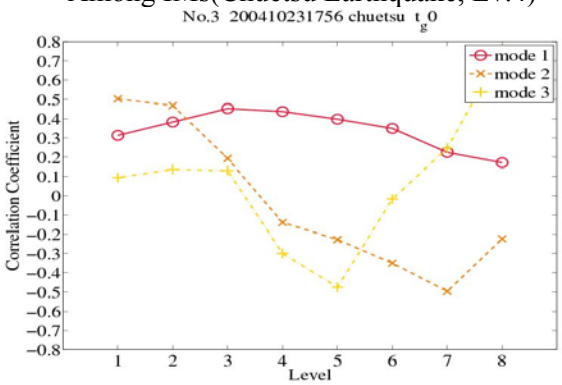

Among Levels(Chuetsu Earthquake, t_{go})

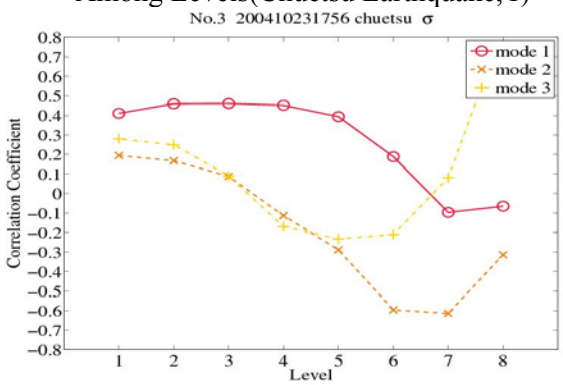

Among Levels(Chuetsu Earthquake, σ_T)

Figure 3.6 Shape of Each Principal Mode

as the bigger the value of I , the smaller the value of tgo, σT and βT, and the bigger the value of γT. It means waves like pulse are apt to have bigger energy than lengthy waves, which was stated above.
This mode is thought to be caused by the fact that the attenuation relations lumps various distances all together. Differently from that, mode 2 is the component as the bigger the value of I , the bigger the value of tgo, σT. The shape of this mode reminds something to do with soil conditions.

Next, looking at the figure for correlation structure among Levels for each IM, the same tendency is shown for I, t_{go} and σ_T. That is, mode 1 is a component as the values moves together upward or downward at all the levels, and mode 2 can be interpreted that the IMs at long-period are dominant or the contrary.

Figure 3.7 and 3.8 are comparisons between the mapping of principal component score of each mode and that of AVS30. AVS30 is the average shear-wave velocities of upper 30 m, an indicator of soil strength proposed by NEHRP. Talking about the relation between the residual of IMs, the mapping of the score of mode 2 at Level 4 (Figure3.7) seems to be most similar to that of AVS30 within near region from the fault of the 3. As for predominant preiod, the score mapping of mode1 for I seems to have much to do with soil conditions. That for t_{go} also seems to be associated in some way with AVS30, the relationship of which is not as clear as that for I.

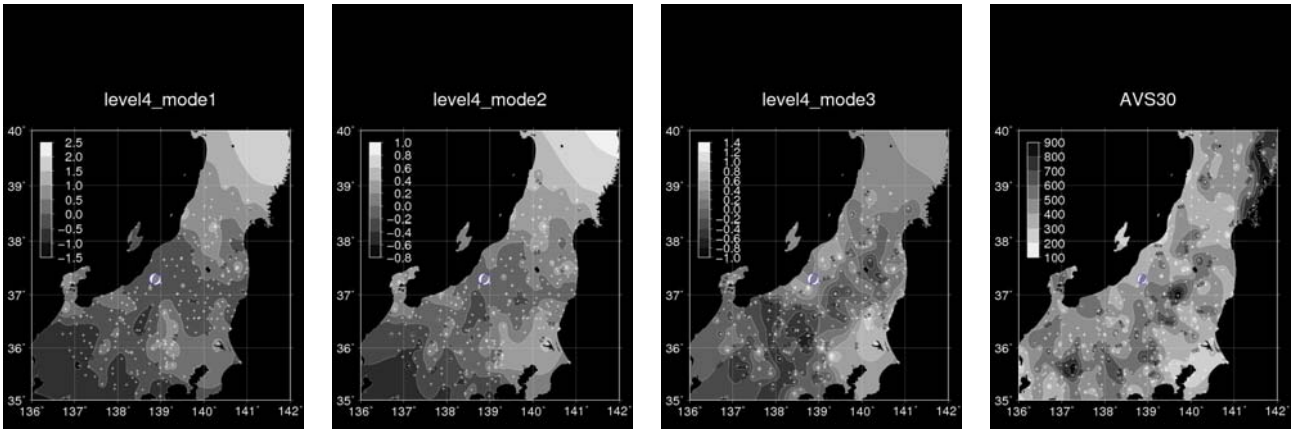

Mode 1 Mode 2 Mode 3 AVS30

Figure 3.7 Mappings of Principal Component Score(Chuetsu Earthquake, Lv.4) and AVS30

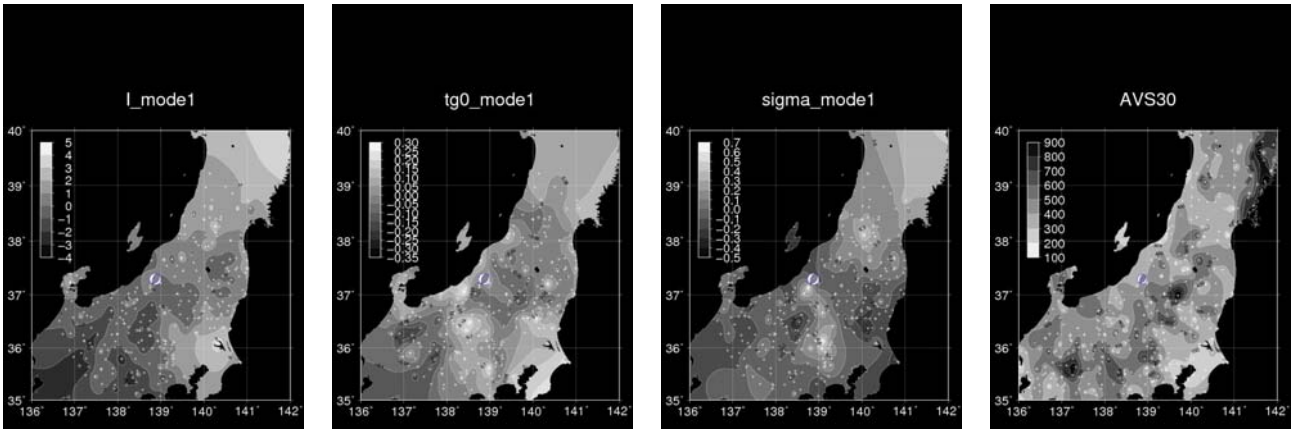

I t_{go} σ_T AVS30

Figure 3.8 Mappings of Principal Component Score (Chuetsu Earthquake, I) and AVS30

4. Conclusion

Modeling band-limited RMS envelope simply by intensity measure and temporal measures simply, the relationships between IMs characterizing waveform envelope and hypo central distance were examined for each

level by regression analysis. The dependence property on earthquake type should be examined and the predictive values of IMs had better be described as the function of magnitude and distance. Correlation structures among levels and among IMs were analyzed by principal component analysis and the tendencies of the shapes of principal modes are obtained. And it was shown the perspective that the correlation structure of residuals can be explained with physical quality such as soil conditions to some extent by plotting the principal component scores on maps.
There is still room for improvement in the way of Modeling waveform. And it is necessary to examine quantitatively the relationship between principal component score and parameters which indicate soil conditions, directivity effect and other properties. And the study about relationship between each principal component and dynamic elastic-plastic response is an issue in the future.

REFERENCES

K-net : http://www.k-net.bosai.go.jp/k-net/

KiK-net : http://www.kik.bosai.go.jp/kik/

Schnabel Per B., Lysmer John and Seed H. Bolton. (1972). "SHAKE", a computer program for earthquake response analysis of horizontally layered site, *EERC*

Iyama J. and Kuwamura J. (1998). time-frequency analysis of earthquake ground motions by wavelet transform, *Journal of Structural and Construction Engineering, AIJ,* **514**, 59-61

I. Daubechies. (1992). Ten lectures on wavelets, Society. for industrial and applied mathematics, Philadelphia

Saito T., Sato H., Ohtake M. and Obara K. (2005). Unified explanation of envelope. broadening and maximum-amplitude decay of high-frequency seismograms based on. the envelope simulation using the Markov approximation: Forearc side of the volcanic front in northeastern Honshu, Japan, *J. Geophys.* **110**, B01304

Takada T. and Ohbuchi M. (2005). Joint PDF of ground motion intensity and duration time, and its applications, *Journal of Structural and Construction Engineering, AIJ,* **589**, 73-80

Uchiyama Y. and Midorikawa S. (2006). Evaluation of amplification factor of site classes based on strong motion records and nonlinear response analysis, *Journal of Structural and Construction Engineering, AIJ,* **571**, 87-93

Uchiyama Y. and Midorikawa S. (2006). Evaluation of amplification factor of site classes based on strong motion records and nonlinear response analysis, *Journal of Structural and Construction Engineering, AIJ,* **571**, 87-93